

# LONGITUDINAL-PHASE-SPACE MANIPULATION FOR EFFICIENT BEAM-DRIVEN STRUCTURE WAKEFIELD ACCELERATION\*

W. H. Tan<sup>1†</sup>, P. Piot<sup>1,2</sup>, A. Zholents<sup>3</sup>

<sup>1</sup> Northern Illinois University, DeKalb, IL 60115, USA

<sup>2</sup> Fermi National Accelerator Laboratory, Batavia, IL 60510, USA

<sup>3</sup> Argonne National Laboratory, Lemont, IL 60439, USA

## Abstract

Collinear beam-driven structure wakefield acceleration (SWFA) is an advanced acceleration technique that could support the compact generation of high-energy beams for future multi-user x-ray free-electron-laser facilities [1]. Producing an ideal shaped drive beam through phase space manipulation is crucial for an efficient SWFA. Controlling the final longitudinal-phase space of the drive beam necessitate staged beam manipulations during acceleration. This paper describes the preliminary design of an accelerator beamline capable of producing drive beam with tailored current distribution and longitudinal-phase-space correlation. The proposed design is based on simple analytical models combined in a 1-D longitudinal beam-dynamics simulation tracking program supporting forward and backward (time reversal) tracking.

## INTRODUCTION

Collinear beam-driven wakefield acceleration (SWFA) achieves high accelerating gradient with a smaller physical footprint than conventional accelerators. The transformer ratio  $\mathcal{R} = \left| \frac{E_+}{E_-} \right|$ , defined as the ratio of the maximum of the accelerating field behind the bunch  $E_+$ , to the maximum of the decelerating field within the bunch  $E_-$ , quantifies the efficiency of beam-driven acceleration. According to the beam loading theorem,  $\mathcal{R} < 2$  for a symmetric longitudinal current distribution. However, it was recognized that tailoring the current distribution could enhance the transformer ratio to arbitrarily large values [2], although at the expense of a reduced peak accelerating electric field [3]. Over the years, several beam shaping techniques have been proposed and investigated including photocathode laser shaping techniques [4–6], transverse-to-longitudinal phase-space emittance exchange [7, 8], and multi-frequency linacs [9]. Most of the shaping schemes (except for the transverse-to-longitudinal phase-space-exchange technique) are based on manipulation within the longitudinal degree of freedom only and can be assisted by collective effects acting in the longitudinal phase space (LPS). Hence, the transverse beam dynamics can be ignored at the early design stage of the bunch-shaping optimization process. Here we report our recent efforts in LPS manipulation to produce an optimized

driver beam for SWFA. We start with the ideal current distribution required for the SWFA. We employ backward tracking technique [4] using the LPS macroparticle-tracking code TWICE [10] to investigate the current distribution needed from the electron gun. The accelerator configuration was obtained through purposeful manual tuning of a generic accelerator layout supplemented with multi-objective optimization.

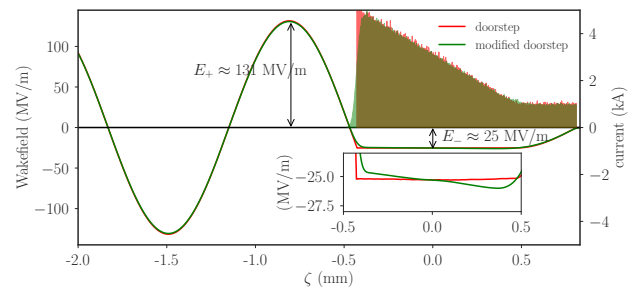


Figure 1: Longitudinal wakefields generated by an exact doorstep bunch (red-shaded area) and a modified doorstep bunch (green-shaded area) as the bunch passes through a 220 GHz corrugated waveguide [11]. The achieved transformer ratio is  $\mathcal{R} \approx 5$ .

## SIMULATION MODEL

### Single Particle Dynamics

The single particle dynamics of an electron beam in relativistic regime, is described by a simple LPS coordinate transformation  $(\zeta_i, E_i) \rightarrow (\zeta_f, E_f)$ . The acceleration through a radiofrequency (RF) linac is assumed to only affect the energy so that  $(\zeta_i, \zeta_f) \rightarrow (\zeta_f = \zeta_i, E_f = E_i \pm eV_{RF} \cos(\phi - \frac{2\pi f}{c} \zeta_i))$ , where  $eV_{RF}$  is the accelerating voltage, and  $f$  and  $\phi$  are the operating frequency and phase associated with the linac. Likewise, an arbitrary longitudinal transformation in a longitudinally-dispersive section is modelled by the transformation  $(\zeta_i, \zeta_f) \rightarrow (\zeta_f = \zeta_i \pm (R_{56}\delta_i + T_{566}\delta_i^2), E_f = E_i)$  where  $\delta_i \equiv \frac{E_i - E_{ref}}{E_{ref}}$  is the relative momentum offset. The + sign indicates forward tracking, conversely the - sign indicates backward tracking. The indices  $i$  and  $f$  are used to describe LPS coordinates before and after the transformation, which it can be either forward or backward tracking.

### Collective Effects

The treatment of collective effects is implemented as a  $\zeta$ -dependent energy-kick approximation on the beam  $\Delta E(\zeta_i)$

\* This work is supported by the laboratory-directed R&D program at ANL via the U.S. Department of Energy, Office of Science, under contract No. DE-AC02-06CH11357 and by the U.S. DOE award No. DE-SC0018656 at NIU.

† z1829753@students.niu.edu

with  $E_i(\zeta_i) \rightarrow E_f(\zeta_i) = E_i(\zeta_i) \pm \Delta E(\zeta_i)$  and  $\zeta_i \rightarrow \zeta_f = \zeta_i$ . The collective effects that we have taken in account includes wakefield modelled by user-defined Green's function, coherent synchrotron radiation (CSR) implemented as a one-dimensional steady-state model [12, 13], and longitudinal space charge (LSC) described by an impedance model [14]. The latter LSC impedance model requires the transverse beam size which, as in the present studies, is estimated from simple consideration but nevertheless provides a starting point to estimate the desired initial distribution along with the linac configuration required.

### Doorstep Distribution

A recent study indicates that adaptive energy chirp is required to circumvent the beam-breakup instability [15]. The doorstep distribution proposed by Bane et al., with further modification on its linear ramp and both ends, results in a linear variation of wakefield within the bunch, allowing us to dynamically control the drive bunch's chirp as it travels the corrugated waveguide, as shown in Fig. 1(inset). The modified doorstep profile optimized following the parameterization

$$I(u) = I_0 S(u) (1 - \text{erf}(16\pi(u_0 - u))) \text{ where,} \quad (1)$$

$$S(u) = \begin{cases} (d_1 + 2\pi(0.75 - u))(1 + d_2(1 - u)^{1.25}) & u \in \text{I,} \\ (1 + 2\pi(0.75 - u))(1 + d_3(1 - u)^{1.25}) & u \in \text{II,} \\ 1 + d_4(d_5 - u)^2 & u \in \text{III,} \\ 1 & u \in \text{IV,} \\ 0 & \text{elsewhere,} \end{cases}$$

where the parameters  $u_0$  and  $d_i$  are constants. Here  $u \equiv \zeta/\lambda$  is the longitudinal position normalized to the fundamental-mode wavelength of the SWFA. The constant and boundaries of the piece-wise regions (I, II, III, IV) are optimized to maximize the transformer ratio and precisely control the linear chirp imparted on the drive bunch. A 10-nC "modified doorstep" distribution with parameters given in Table 1 appears in Fig 2.

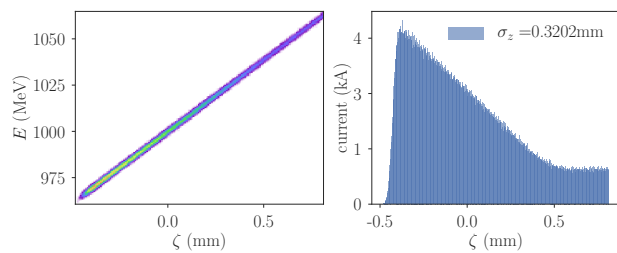


Figure 2: LPS (left) and current (right) distributions at the end of beamline.

### Beamline

We use a widely adopted linac architecture used in XFELs shown in Fig. 3. Given the required high charge and anticipated long bunch out of the photoinjector, our linac consists of two 650 MHz superconducting accelerating cryomodules

Table 1: Parameters Associated with the Modified Doorstep Distribution

Bunch Property	Value	Value
Number of macroparticles	100 593	--
Charge	10	nC
Reference energy	1	GeV
Rms length	320.3	$\mu\text{m}$
Rms fractional energy spread	2.48	%
Rms fractional slice energy spread	0.1	%

(shown as L1 and L2), with a 3.9 GHz harmonic linearizer (L39), together with two bunch compressors (shown as BC1 and BC2). Since a positive chirp is required for SWFA (the bunch head has higher energies), we need  $R_{56} < 0$  to compress the bunch. Hence the second bunch compressor is moved to the end of the linac. It also enables the use of a longer bunch in the linac and reduces collective effects. We model the bunch compressors with  $R_{56}$  and  $T_{566}$ . For chicane-like compressor (as currently considered), we divide a compressor in two sections with same  $R_{56}$  and  $T_{566}$ , where such an approximation is valid for the  $R_{56}$  as long as the compressor is symmetric with respect to its midpoint but it is generally not applicable to the  $T_{566}$ . The CSR energy kicks are applied in each section after the dipole magnets. We assume all dipole magnets to be 40-cm long with a  $8^\circ$  bending angle.



Figure 3: Diagram of the linac used in the simulations to produce the tailored bunch. L1 and L2 are 650 MHz linacs, L39 is a 3.9-GHz linac, and BC1 and BC2 are magnetic bunch compressors.

## SIMULATION AND OPTIMIZATION

We employed forward and backward tracking simulation to study the LPS manipulation for producing an ideal current distribution. With a well-defined distribution shown in Fig. 2, backward tracking simulation using the beamline from Fig. 3 allows us to estimate the target distribution required from a photoinjector. After obtaining an initial distribution at the beginning of the beamline, we checked the beam parameters to investigate the feasibility of it to be produced from a photoinjector, and beamline parameters to produce it. The process is iterated to fine-tune the beamline parameters. Additionally, we modify the initial distribution to eliminate unusual discontinuity in LPS and assess the impact of these alterations on the final distribution. We employed multi-objective optimization using DEAP framework [16] to optimize the accelerator parameters with self-defined constraints. An electron gun coupled to a short linac, would precede our beamline, and hence imposes constraints on beam parameters. The initial distribution needs to

Content from this work may be used under the terms of the CC BY 3.0 licence (© 2019). Any distribution of this work must maintain attribution to the author(s), title of the work, publisher, and DOI

have a peak current lower than 300 A, a mean energy lower than 70 MeV, a full energy spread lower than 10% and a total bunch length smaller than 4 cm. We also require that the energy chirp of the beam has the same sign before BC1 and at the beginning of L1.

To translate such conditions into objective functions for optimization, we did a polynomial fitting of LPS  $\delta = c_0 + c_1\zeta + c_2\zeta^2 + c_3\zeta^3$  and minimized  $c_2/c_1$  before BC1 and before L1.

## RESULTS AND DISCUSSION

The optimized accelerator parameters are summarized in Table 2 and initial distribution obtained from these settings with backward tracking are shown in the upper plot of Fig 4. The initial LPS is dominated by the linear correlation of  $(\zeta, E)$ . Removing its linear chirp revealed its highly nonlinear part at the tail edge of the beam, as shown in the right panel of Fig 4.

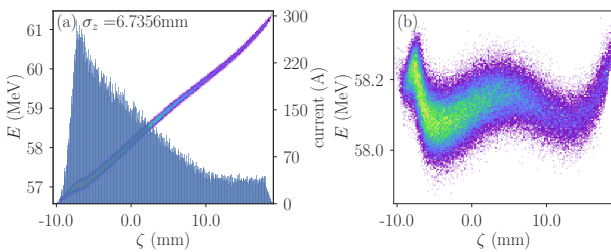


Figure 4: Initial bunch LPS with its current distribution (a), and its LPS after removing linear chirp (b).

We manually altered its tail edge to make it smoother, as shown in Fig. 5(a) and performed forward tracking with the same parameters to check the final distribution produced. The result, shown in Fig. 5(c), differs from the ideal distribution in Fig. 2, as expected from our modification. However, through the use of masks in the middle of BC1, we can further shape the bunch to match the ideal distribution. The comparison of final distributions, with and without applying masks, with generated wakefields as the beam passes through a corrugated waveguide, is shown in Fig. 6. The beam loss after applying a mask for dispersive collimation is 6.8%. The differences in wakefields play an important role in the beam transverse dynamics.

The modified initial distribution [Fig. 5(a)] will need to be generated from a photoinjector. Such an effort is presently underway. The fast oscillation visible in Fig. 5(b) can be introduced using a corrugated pipe [17].

## CONCLUSION

Using TWICE backward-tracking capabilities we have optimized the longitudinal dynamics associated with an SRF linac capable of producing drive bunches with current distributions needed for efficient excitation of wakefields in SWFAs. The backward-tracking technique was combined with forward tracking and optimization tools to explore possible initial distributions that need to be produced by the

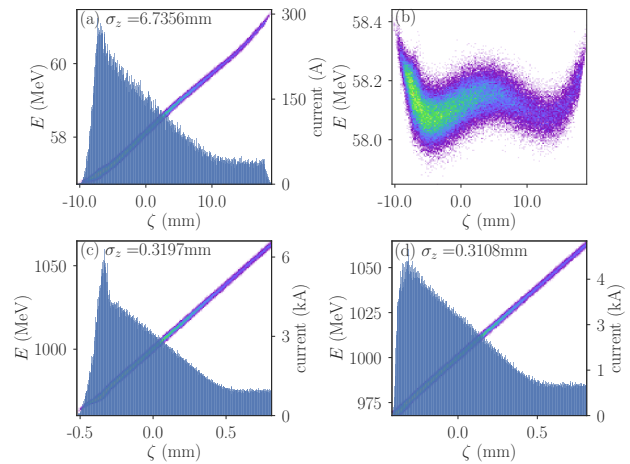


Figure 5: Modified-bunch LPS and current distribution (a), and LPS after removing the linear chirp (b). Final bunch after forward tracking without (c) and with dispersive collimation in BC1 (d).

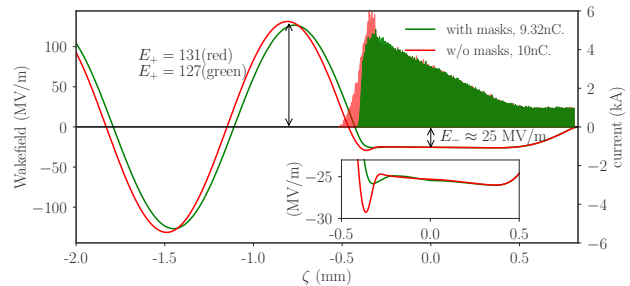


Figure 6: Comparison of generated wakefields from final bunches, the beam loss after dispersive collimation (green-shaded area).

Table 2: Optimized Accelerator Parameters

Parameter	Value	Unit
Accelerating voltage L1	209	MV
Phase L1	18	deg
Frequency L1	650	MHz
Accelerating voltage L39	7	MV
Phase L39	219	deg
Frequency L39	3.9	GHz
$R_{56}$ for bunch compressor 1 (BC1)	-0.16	m
$T_{566}$ for bunch compressor 1 (BC1)	0.22	m
Accelerating voltage L2	850	MV
Phase L2	28	deg
Frequency L2	650	GHz
$R_{56}$ for bunch compressor 2 (BC2)	-0.14	m
$T_{566}$ for bunch compressor 2 (BC2)	-0.25	m

photoinjector. The optimized accelerator configuration will guide the design of the bunch compressors and photoinjector, before proceeding with full-fledged simulations including the transverse beam dynamics.

## REFERENCES

- [1] A. Zholents, W. Gai, S. Doran, R. Lindberg, J. G. Power, N. Strelnikov, Y. Sun, E. Trakhtenberg, I. Vasserma, C. Jing, A. Kanareykin, Y. Li, Q. Gao, D. Y. Shchegolkov, and E. I. Simakov, "A preliminary design of the collinear dielectric wakefield accelerator," *Nucl. Instrum. Methods Phys. Res., Sect. A*, vol. 829, pp. 190 – 193, 2016.
- [2] K. L. Bane, P. Chen, and P. B. Wilson, "On collinear wake field acceleration," *Proc. of the 1985 Part. Accel. Conf. (PAC1985): Accelerator Engineering and Technology Vancouver, BC May 13-16, 1985*, vol. 32, pp. 3524–3526, 1985.
- [3] S. S. Baturin and A. Zholents, "Upper limit for the accelerating gradient in the collinear wakefield accelerator as a function of the transformer ratio," *Phys. Rev. Accel. Beams*, vol. 20, p. 061302, June 2017.
- [4] M. Cornacchia, S. Di Mitri, G. Penco, and A. A. Zholents, "Formation of electron bunches for harmonic cascade x-ray free electron lasers," *Phys. Rev. Spec. Top. Accel Beams*, vol. 9, p. 120701, Dec. 2006.
- [5] G. Penco, M. Danailov, A. Demidovich, E. Allaria, G. De Ninno, S. Di Mitri, W. M. Fawley, E. Ferrari, L. Giannessi, and M. Trovó, "Experimental Demonstration of Electron Longitudinal-Phase-Space Linearization by Shaping the Photoinjector Laser Pulse," *Phys. Rev. Lett.*, vol. 112, p. 044801, Jan. 2014.
- [6] F. Lemery and P. Piot, "Tailored electron bunches with smooth current profiles for enhanced transformer ratios in beam-driven acceleration," *Phys. Rev. Spec. Top. Accel Beams*, vol. 18, p. 081301, Aug. 2015.
- [7] B. Jiang, C. Jing, P. Schoessow, J. Power, and W. Gai, "Formation of a novel shaped bunch to enhance transformer ratio in collinear wakefield accelerators," *Phys. Rev. Spec. Top. Accel Beams*, vol. 15, p. 011301, Jan. 2012.
- [8] G. Ha, M. H. Cho, *et al.*, "Precision control of the electron longitudinal bunch shape using an emittance-exchange beam line," *Phys. Rev. Lett.*, vol. 118, p. 104801, 2017.
- [9] P. Piot, C. Behrens, C. Gerth, M. Dohlus, F. Lemery, D. Mihalcea, P. Stoltz, and M. Vogt, "Generation and Characterization of Electron Bunches with Ramped Current Profiles in a Dual-Frequency Superconducting Linear Accelerator," *Phys. Rev. Lett.*, vol. 108, p. 034801, Jan. 2012.
- [10] W. Tan, P. Piot, and A. Zholents, "Longitudinal beam-shaping simulation for enhanced transformer ratio in beam-driven accelerators," in *2018 IEEE Advanced Accelerator Concepts Workshop (AAC)*, pp. 1–5, Aug 2018.
- [11] G. Waldschmidt *et al.*, "Design and Test Plan for a Prototype Corrugated Waveguide," in *Proc. 9th International Particle Accelerator Conference (IPAC'18), Vancouver, BC, Canada, April 29-May 4, 2018*, no. 9 in International Particle Accelerator Conference, (Geneva, Switzerland), pp. 1550–1552, JACoW Publishing, June 2018.
- [12] E. L. Saldin, E. A. Schneidmiller, and M. V. Yurkov, "On the coherent radiation of an electron bunch moving in an arc of a circle," *Nucl. Instrum. Methods Phys. Res., Sect. A*, vol. 398, no. 2, pp. 373 – 394, 1997.
- [13] C. E. Mitchell, J. Qiang, and R. D. Ryne, "A fast method for computing 1-D wakefields due to coherent synchrotron radiation," *Nucl. Instrum. Methods Phys. Res., Sect. A*, vol. 715, pp. 119 – 125, 2013.
- [14] J. Qiang, R. D. Ryne, M. Venturini, A. A. Zholents, and I. V. Pogorelov, "High resolution simulation of beam dynamics in electron linacs for x-ray free electron lasers," *Phys. Rev. Spec. Top. Accel Beams*, vol. 12, p. 100702, Oct. 2009.
- [15] S. S. Baturin and A. Zholents, "Stability condition for the drive bunch in a collinear wakefield accelerator," *Phys. Rev. Accel. Beams*, vol. 21, p. 031301, Mar. 2018.
- [16] F.-A. Fortin, F.-M. De Rainville, M.-A. Gardner, M. Parizeau, and C. Gagné, "DEAP: Evolutionary algorithms made easy," *Journal of Machine Learning Research*, vol. 13, pp. 2171–2175, July 2012.
- [17] Z. Zhang, K. Bane, Y. Ding, Z. Huang, R. Iverson, T. Maxwell, G. Stupakov, and L. Wang, "Electron beam energy chirp control with a rectangular corrugated structure at the linac coherent light source," *Phys. Rev. Spec. Top. Accel Beams*, vol. 18, p. 010702, Jan 2015.